STEMedicine

RESEARCH ARTICLE

Hsa_circ_0002111/miR-557/DUSP14 axis mediates euthyrox-resistance in papillary thyroid cancer

Jing Zhou†, Jing Liu†, Weiyuan Ma and Pengxin Zhao*

The Second Hospital of Hebei Medical University, Shijiazhuang, Hebei, China

Abstract

As one of the most commonly used chemotherapeutic drug for papillary thyroid cancer (PTC), euthyrox affects the therapeutic outcome due to the resistance of euthyrox. Hsa_circ_0002111 is highly expressed in euthyrox-resistant PTC patients, and this study intends to explore its role in euthyrox drug resistance. PTC patient samples were used to screen for Circ_0002111 expression. TPC-1 and K1 PTC cell lines and their corresponding euthyrox-resistant cell lines (TPC-1/euthyrox and K1/euthyrox), and a benign human thyroid follicular cell line (Nthy-ori 3-1) were used in *in vitro* experiments. Circ_0002111 was knocked down in euthyrox-resistant cell lines, and cell viability and colony formation were detected. Caspase-3 activity assay and nucleosomal fragmentation assay were used for the detection of apoptosis. Luciferase reporter assay and biotin-labeled RNA pulldown assay were used to analyze interactions between Circ_0002111 and miR-557, or miR-557 and DUSP14. The upregulation of Circ_0002111 was found in PTC patient samples and associated with euthyrox-resistance in poor prognosis of PTC patients. Experiments in cell lines showed that Circ_0002111 regulates euthyrox-resistance in PTC cells. Mechanistic studies showed that Circ_0002111 promoted DUSP14 expression through miR-557, and euthyrox-resistance in PTC cells depended on the regulation via miR-557/DUSP14 signaling pathways. In conclusion, Hsa_circ_0002111 promotes euthyrox-resistance of PTC cells by adsorption miR-557 upregulation, suggesting Circ_0002111 might be a potential diagnostic marker and therapeutic target for euthyrox-resistant PTC patients.

Keywords: *miR-557*; *Circ_0002111*; *Euthyrox resistant*; *DUSP14*; *Umael*

Received: 10 March 2022; Revised: 15 March 2022; Accepted: 15 March 2022; Published: 4 April 2022

Thyroid cancer (TC) is the most common endocrine system malignant tumor. Though early screening has been spread to prevent TC, the percentile of TC patient is keeping rising. Papillary, follicular, medullary, and intervariant are the commonly found TC subtypes (1, 2), among which the papillary thyroid carcer (PTC) is the most common one, and PTC patients account for more than 80% of all TC patients (3). PTC usually has a better prognosis, but in some patients, especially with low differentiation, prognosis with malignant pathological features such as lymph node and distal metastasis is not satisfactory (4–6). Euthyrox has become one of the most commonly used chemotherapeutic drugs because of its high efficiency, low side effect, and convenience (7). However, some PTC patients have euthyrox-resistance during treatment that affects the clinical outcome, and it is important to clarify the underlying mechanism to facilitate the use of euthyrox.

Screening in samples of PTC patients found that Hsa_circ_0002111 expression was obviously increased, especially in PTC patients with euthyrox-resistance during treatment because circular RNAs (circ RNAs) play important roles in cell growth, signal transduction, and physiological and pathological responses (8–10). The role of circRNAs in tumors has become a hot spot in recent years (11–13). The circular RNA Hsa_circ_0002111 that found in this study has never been reported before. In this study, we intended to explore its expression pattern and investigate its functional mechanism in PTC euthyrox-resistance.

†These authors contributed equally to this paper.

Materials and methods

Patient samples

Fifty tumor tissue samples and 50 normal adjacent tissues from 50 PTC patients were obtained. The study protocol was approved by the Second Hospital of Hebei Medical University. All participants gave their written consent.

Cell lines

TPC-1 and K1, euthyrox-resistant TPC-1 cells (TPC-1/euthyrox), and euthyrox-resistant K1 cells (K1/euthyrox) were provided by ATCC. Nthy-ori3-1 cell line was provided by Shanghai Liangtai Biotech. The cells were routinely cultured in RPMI1640 medium (Thermo Fisher Scientific) with 10% fetal bovine serum (FBS, Takarabio, Japan), and common cell culture supplies.

qRT-PCR

RNA was extracted using AllPrep DNA/RNA Kits (Cat. 80204) and transcribed using the QuantiNova Reverse Transcription Kit (Cat. 205413). Quantitative reverse transcription polymerase chain reaction (qRT-PCR) was conducted using the QuantiTect SYBR Green PCR Kit (Cat. 204143), following the manufacturer's instruction. The primers used are shown as follows:

Circ_0002111 primer:
Forward: CCCAGATACCATTGCTTCACA;
Reverse: CAACACCCTCATTTACCCCTT.

GAPDH (internal control gene) primer:
Forward: AGGTCGGTGTGAACGGATTTG;
Reverse: GGGGTCGTTGATGGCAACA.

miR-557 primer:
5'-CTCAACTGGTGTCGTGGAGTCGGCAATTCAGTTGAGAGACAAGG-3' (stemloop primer), 5'-ACACTCCAGCTGGGGTTTGCACGGGTGGGC-3' (forward) and 5'-TGGTGTCGTGGAGTCG-3' (reverse).

U6 primer:
Forward: 5'-GCTTCGGCAGCACATATACTAAAAT-3';
Reverse: 5'-GAATTTCCTGCTTGAGCCGC-3'.

DUSP14 primer:
Forward: GGACTCTTGAGGAAGAAGGAGAC;
Reverse: GGAATAGAGAGGAGGTGATTTGAG.

GAPDH (internal control gene) primer:
Forward: AGGTCGGTGTGAACGGATTTG;
Reverse: GGGGTCGTTGATGGCAACA.

Western blot

Tissues were collected and put into lysis buffer containing protease inhibitor cocktail to lyse the protein. Protein levels were then determined, and then the protein was heated at 100°C for 5 min to denature. Sodium dodecyl sulfate–polyacrylamide gel electrophoresis gel was configured with the appropriate concentration, and electrophoresis was performed. Protein marker and protein samples were loaded into the wells of the gel. The appropriate voltage for electrophoresis was selected according to the size of the protein band. After the electrophoresis, the protein gel was taken out into transfer solution, the protein in the gel was transferred to the polyvinylidene fluoride (PVDF) membrane in a box with ice, and then the PVDF membrane was taken out for incubation with antibodies. After incubating for 2 h in 5% skimmed milk, the membrane was treated with the target antibody and shaken overnight at 4°C. In the next day, the target antibody was washed away using tris-buffered saline and Tween-20. According to the target antibody, the appropriate secondary antibody was selected for incubation. After that, chemiluminescence was performed to detect the target protein band. Antibodies used are as follows.

Colony forming assay

After digesting the cell with trypsin, the cell suspension is resuspended with a complete medium (base medium plus 10% fetal bovine serum) and counted. Then, 400–1,000 cells were inoculated in each experimental group in the 6-well plate culture plate (generally 700 cells/well based on cell growth). Cells continued to grow until 14 days or until the number of cells in the vast majority of individual clone was greater than 50, changing medium every 3 days and observe cell status. Afterward, the cells were photographed under a microscope and then washed with phosphate-buffered saline (PBS), and a 1 mL 4% polyformaldehyde fixation was added for 30–60 min per well and washed with PBS. A 1 mL of crystalline purple dye was added to each well for 20 min and then washed with PBS for three times. Pictures were taken for each well after drying, and then the colonies were counted.

Luciferase assay

Mutant and wild-type (wt) sequences were amplified and then inserted into the vectors to construct luciferase reporter plasmids. The sequences used are showed as follows:

Circ_0002111 wt primers:
Forward: CCAA CTCGAG CAATGCTGGGGTGAAAA;
Reverse: CCAA GCGGCCGC TTTCAGCAGATCCTTGGAG.

Circ_0002111mut primers:
Forward: CAAAAGATCAGATGTGGAACCAC;

Reverse: GTGGTTCCACATCTGATCTTTTG.

DUSP14 3'UTR wt primers:
Forward: CCAA CTCGAG TGCCACTGAAGCC TGCGTCAGC;
Reverse: CCAA GCGGCCGC TATGTTAAGCATAT AGATTT.

DUSP14 3'UTRmut primers:
Forward: TGCAGGAGGAGCTCAATACCCAA;
Reverse: TTGGGTATTGAGCTCCTCCTGCA.

The luciferase activities were detected using the dual luciferase reporter kit (Cat. K2062-200, BioVision, USA). The medium was removed followed by PBS wash for twice and then added a minimum volume of 1 × CCLR to cover the cells (250 μL/60 mm petri dish), incubated at room temperature. Scrape the attached cells out of the petri dish and transfer the cells and solutions to the tube. Centrifuge at 12,000 rpm for 5 s and then transfer the cells to a new tube. Mix 20 μL of cell extract with 100 μL luciferase analysis reagent. Place the reaction in a luminometer for 10 s and record data.

Biotin RNA pulldown assay

The RNA pulldown assay was conducted following a protocol as previously described (14). Probes used are as follows:

Circ_0002111-DNA-1-sense:
(biotin-) AATTTTGGAAAAGGAGACCCC;

Circ_0002111-DNA-1-antisense:
(biotin-) GGGGTCTCCTTTTCCAAAATT;

Circ_0002111-DNA-2-sense:
(biotin-) TTTTGATTTTACAGGAATGACGCTGGAT;

Circ_0002111-DNA-2-antisense:
(biotin-) ATCCAGCGTCATTCCTGTAAAATCAAAA;

Circ_0002111-DNA-3-sense:
(biotin-) CCTGTCAGGAGTTCATTGCAAATCTGCA;

Circ_0002111-DNA-3-antisense:
(biotin-) TGCAGATTTGCAATGAACTCCTGACAGG.

Cell transfection

The transfection experiment was conducted following a standard protocol from Santa Cruz Biotechnology. miR-557 mimics (miR-557) and the corresponding miRNA negative control (miR-NC) were provided by Qiagen. The siRNA used are as follows:

si-Circ_0002111#1: GCTTCTTAATACCGATCTACA;
si-Circ_0002111#2:GGAATGACGCTGGATCAGTCA;
si-NC: UUCUCCGAACGUGUCACGUTT.

Nucleosomal fragmentation assay

Induction of apoptosis by enzastaurin (Sigma-Aldrich) was measured by nucleosomal fragmentation. Briefly, cells (5×10^3/well) were plated in 96-well plates, incubated with or without enzastaurin for 72 h.

Other assays

CCK-8 (Cell Counting Kit-8, Dojindo) assay was conducted following the protocol. Caspase-3 activity assay was performed using Caspase-3 Activity Assay Kit (Cell Signaling Technology) following the product protocol exactly. Cytosolic/nuclear fractionation was done according to a reported method (15).

Statistical analysis

Data were presented as means and standard deviation (SD). The difference between more than two groups was performed using the one- or two-way analysis of variance (ANOVA), followed by a Tukey's or Bonferroni post hoc tests. Student's *t*-test was used to assess the difference between two groups. $P < 0.05$ was considered as significant.

Results

Higher expression level of Circ_0002111 in euthyrox-resistant patients' samples and cell lines

Circ_0002111 was found to have higher expression levels in PTC tumor tissue samples (Fig. 1a). Further analysis found that the expression level of Circ_0002111 in the tumor tissue samples of PTC patients with euthyrox-resistance was significantly higher than that of PTC patients with euthyrox-sensitivity (Fig. 1b). Using Kaplan–Meier for a prognostic analysis, we found that patients with high expression levels of Circ_0002111 had lower overall survival rates (Fig. 1c). Furthermore, we examined Circ_0002111 expression levels in two PTC cell lines (TPC-1 and K1), along with their corresponding euthyrox-resistant cell lines (TPC-1/euthyrox and K1/euthyrox) and a benign human thyroid follicular cell line (Nthy-ori 3-1). Circ_0002111 was found to be significantly higher in PTC cell lines than in Nthy-ori 3-1, and the expression level of Circ_0002111 in euthyrox-resistant cell lines was higher than that in their paired cell lines (Fig. 1d).

Hsa_circ_0002111 regulate euthyrox resistance of PTC cells

Then, we explored the effects of Circ_0002111 on euthyrox-resistance of PTC cells. First, we transfected

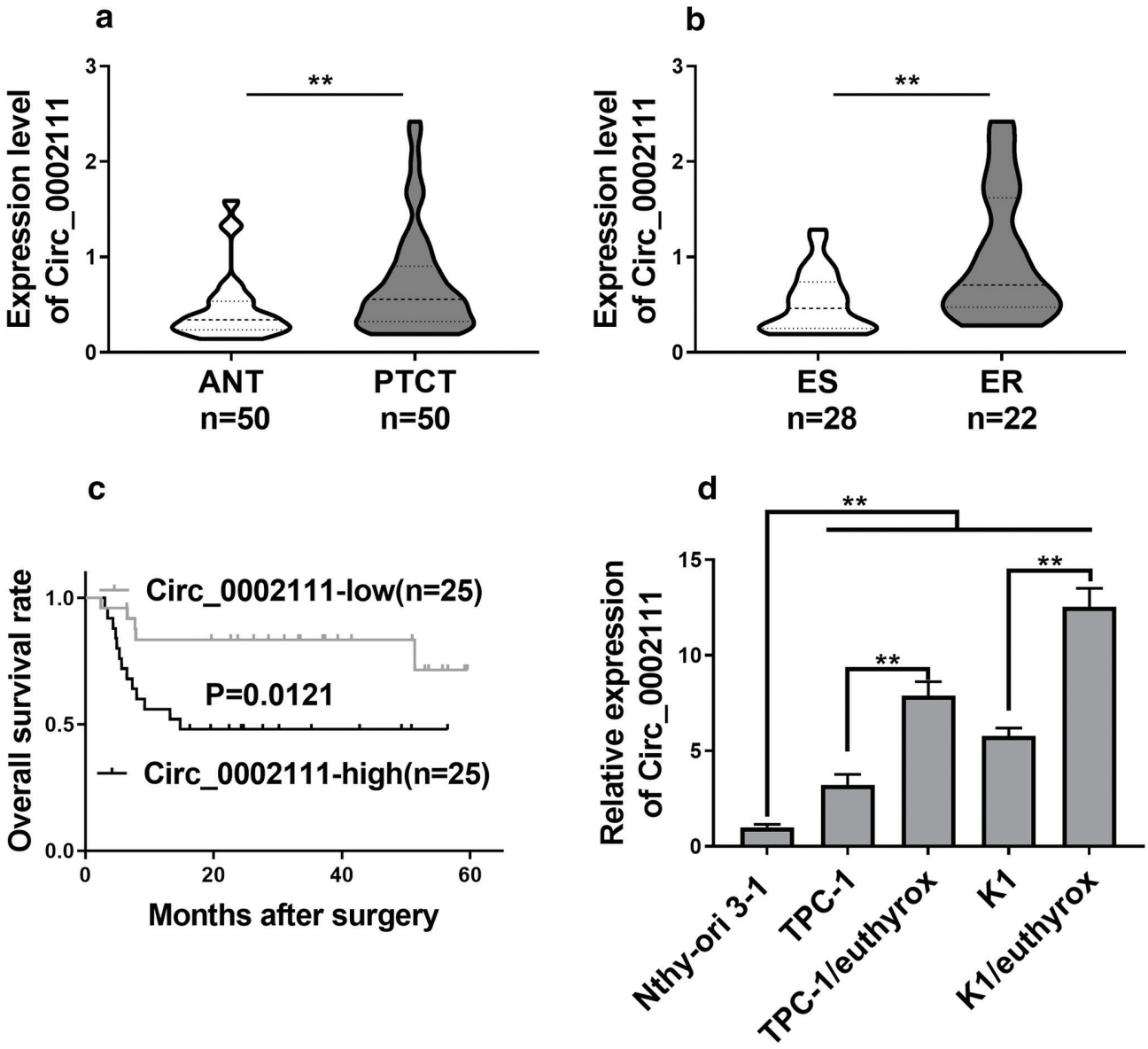

Fig. 1. Elevated Hsa_circ_0002111 was associated with euthyrox-resistance and poor prognosis of PTC patients. (a) Circ_0002111 expression in 50 pairs of PTC tissues (PTCT) and matched adjacent normal thyroid tissues (ANT) were analyzed by qRT-PCR assay. (b) qRT-PCR assay was performed to examine the expression level of Circ_0002111 in PTC tissues from 28 euthyrox-sensitive (ES) PTC patients and 22 euthyrox-resistant (ER) PTC patients. (c) PTC patients with low expression of Circ_0002111 had higher fraction survival compared with PTC patients with high Circ_0002111 expression. (d) qRT-PCR assay was conducted to evaluate Circ_0002111 expression in two PTC cell lines (TPC-1 and K1), their euthyrox-resistant counterparts (TPC-1/euthyrox and K1/euthyrox), and Nthy-ori 3-1. *$P < 0.05$; **$P < 0.01$.

Circ_0002111 siRNA in two euthyrox-resistant cell lines, TPC-1/euthyrox and K1/euthyrox, to knock down the expression of Circ_0002111 (Fig. 2a). Then, a series of functional experiments were carried out. From CCK-8 assay, we found that the survival ability of TPC-1/euthyrox and K1/euthyrox after knockout of Circ_0002111 was significantly reduced with the treatment of different concentrations of euthyrox (Fig. 2b and c). Colonal formation experiments showed that knockout of Circ_0002111 significantly downregulated the proliferation ability of TPC-1/euthyrox and K1/euthyrox cells in vitro after euthyrox treatment (Fig. 2d). Cell apoptosis activity was also upregulated with knockout of Circ_0002111 in both cell lines (Fig. 2e, f). These results showed that knockdown of Circ_0002111 promoted the euthyrox sensitivity of euthyrox-resistant cells.

Hsa_circ_0002111 directly targeted miR-557 in PTC cells

We then sought to find out the mechanism that how Circ_0002111 functions. The sublocation of ring RNA

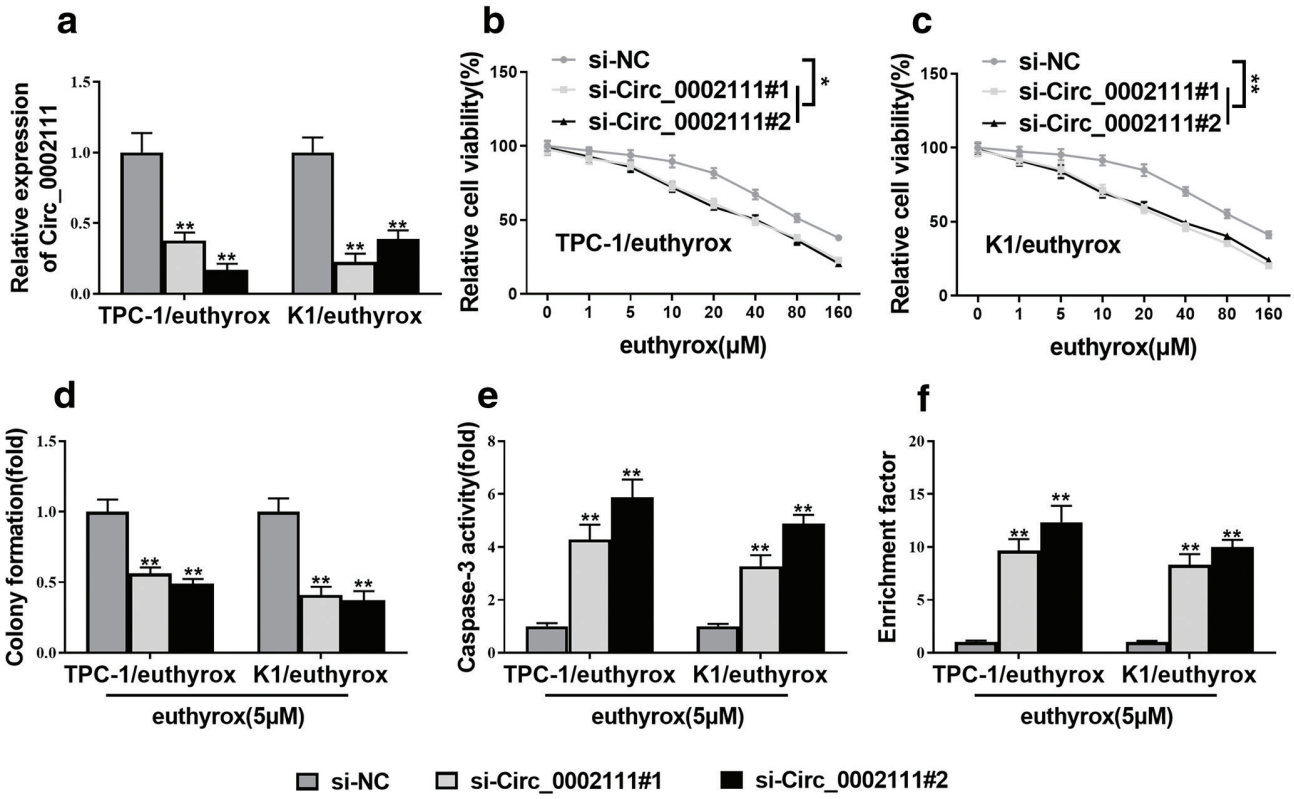

Fig. 2. Hsa_circ_0002111-mediated euthyrox-resistance of PTC cells. (a) Knockdown efficiency of Circ_0002111 in TPC-1/euthyrox and K1/euthyrox cells transfected with si-Circ_0002111#1 and si-Circ_0002111#2 or negative control siRNA (si-NC) was confirmed by qRT-PCR analysis. (b and c) CCK-8 assays were conducted to evaluate the survival rate of Circ_0002111-depleted TPC-1/euthyrox and K1/euthyrox cells treated with different doses of euthyrox for 48 h. (d) Colony formation assay was performed to determine cell proliferation ability of Circ_0002111-depleted TPC-1/euthyrox and K1/euthyrox cells with the treatment of euthyrox (5 μM). (e, f) Cell apoptosis of Circ_0002111-depleted TPC-1/euthyrox and K1/euthyrox cells treated with 5 μM euthyrox was assessed by caspase-3 activity assay and nucleosomal fragmentation assay. $*P < 0.05$; $**P < 0.01$.

in cells largely determines its mode of action, and most ring RNA located in cytoplasm can play as a ceRNA role. Therefore, we first determine the sublocation of the Circ_0002111 in the cell (Fig. 3a, b) and found that Circ_0002111 was mainly distributed in the cytoplasm through the nuclear separation experiment, so we thought that Circ_0002111 could also work through the ceRNA mode. By circular RNA interactome, the functional-related miRNA miR-557 was predicted as that can interact with Circ_0002111 (Fig. 3c). We found the binding site on the Circ_0002111 and mutated the cite to see how they interacted. The double fluorescence report experiment proved that the miR-557 could act on the wild type Circ_0002111 but could not act on the mutant Circ_0002111 (Fig. 3d, e). Through the biotin labeled RNA pulldown experiment, we found that the Circ_0002111 and miR-557 could be directly combined (Fig. 3f, g). Furthermore, upon knock-down of Circ_0002111, the miR-557 level was significantly upregulated (Fig. 3h). These results demonstrated that Circ_0002111 could interact with miR-557 and downregulate the miR-557 expression level in euthyrox-resistant PTC cells.

Hsa_circ_0002111 interacted with miR-557 to upregulate DUSP14 expression

Then, we wanted to find miR-557 downstream target. Through Targetscan, we predicted the potential functional-related target for miR-557: DUSP14 (Fig. 4a). Then, we found the binding sites of DUSP14 for miR-557, and the binding sites were mutated to construct fluorescence reporting vector. The results of double fluorescence report system showed that miR-557 could act on wild type DUSP14 by 3'UTR but could not combine the mutated DUSP14 3'UTR (Fig. 4b, c). Through qRT-PCR and Western blotting, we proved that the overexpression of miR-557 can inhibit the expression of DUSP14 (Fig. 4d, e). We further explored the relationship between Circ_0002111 and DUSP14 expressions, and the DUSP14 expression level was downregulated after knocking down the Circ_0002111 (Fig. 4f, g). These results showed that Circ_0002111 and

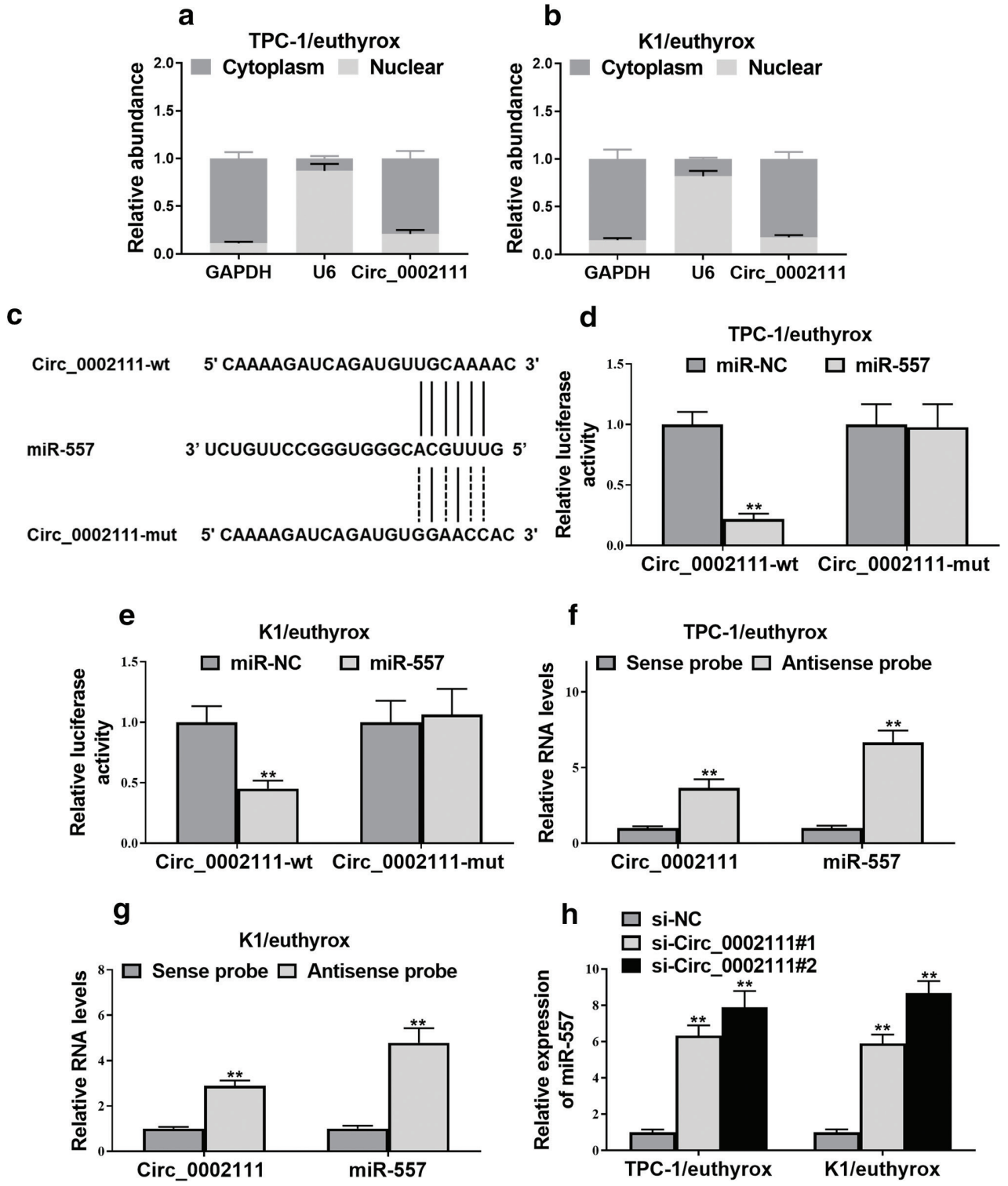

Fig. 3. Hsa_circ_0002111 directly targeted miR-557 in PTC cells. (a, b) Subcellular fractionation of TPC-1/euthyrox and K1/euthyrox cells and measurement of Circ_0002111 by qRT-PCR analysis. (c) Diagrammatic sketch showed the wild-type (Circ_0002111-wt) and mutant (Circ_0002111-mut) potential binding sites of miR-557 in Circ_0002111 transcripts. (d, e) Luciferase assay of TPC-1/euthyrox and K1/euthyrox cells cotransfected with miR-557 mimics and a luciferase reporter containing wild-type or mutant Circ_0002111 constructs. (f, g) Enrichment of Circ_0002111 and miR-557 in biotin-labeled anti-Circ_0002111 probes pull-down RNA fraction of TPC-1/euthyrox and K1/euthyrox cells was determined by qRT-PCR. (h) qRT-PCR analysis of the relative expression of miR-557 in TPC-1/euthyrox and K1/euthyrox cells transfected with si-Circ_0002111#1 and si-Circ_0002111#2 or negative control siRNA (si-NC). $*P < 0.05$; $**P < 0.01$.

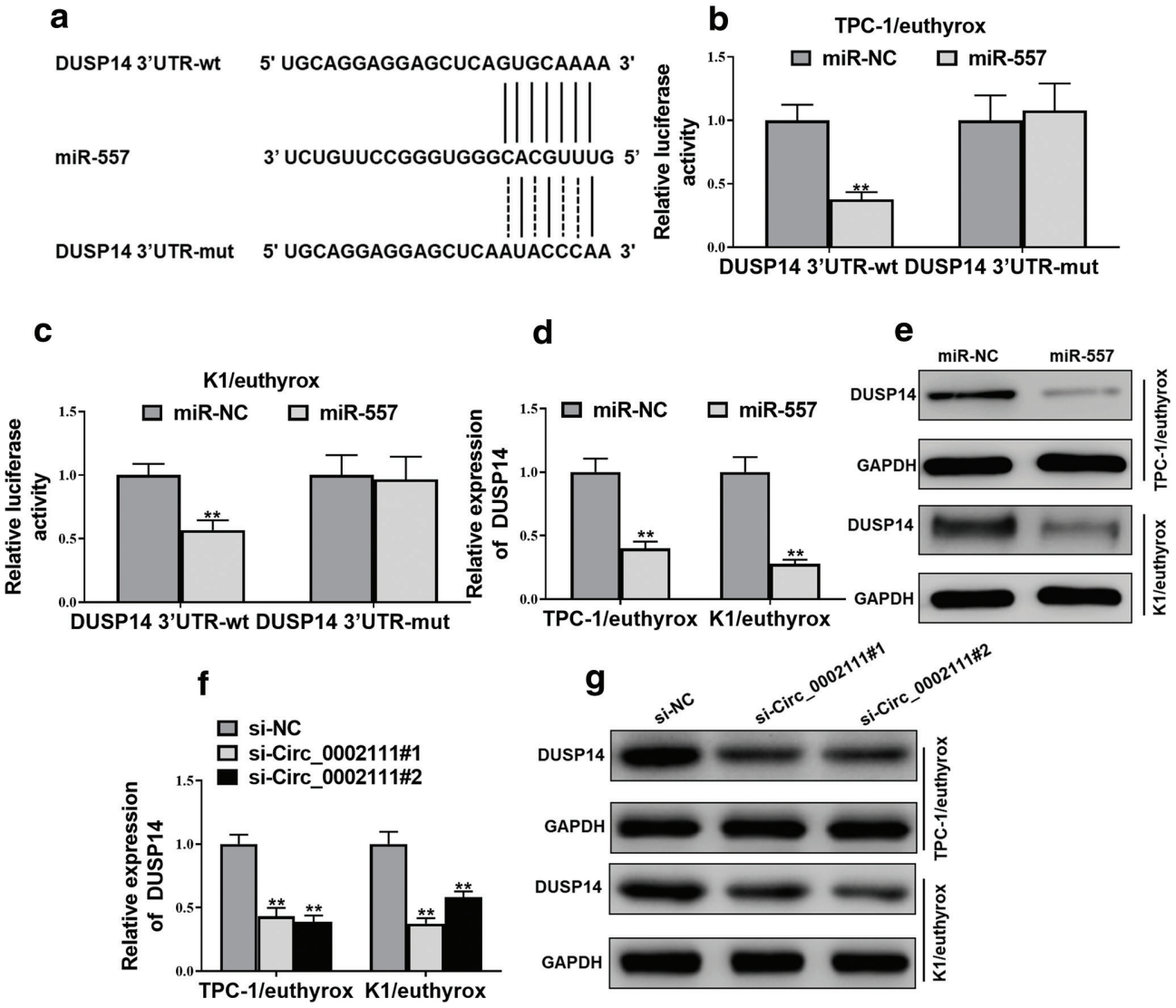

Fig. 4. Hsa_circ_0002111 acted as a 'sponge' of miR-557 to upregulate DUSP14 expression. (a) Diagrammatic sketch showed the wild-type (DUSP14 3'UTR-wt) and mutant (DUSP14 3'UTR-mut) potential binding sites of miR-557 in DUSP14 3'UTR. (b, c) Luciferase assay of TPC-1/euthyrox and K1/euthyrox cells cotransfected with miR-557 mimics and a luciferase reporter containing wild-type or mutant DUSP14 3'UTR constructs. (d, e) mRNA and protein levels of DUSP14 in TPC-1/euthyrox and K1/euthyrox cells transfected with miR-557 mimics (miR-557) or negative control miRNA mimics (miR-NC) were determined by qRT-PCR and Western blot, respectively. (f, g) mRNA and protein levels of DUSP14 in TPC-1/euthyrox and K1/euthyrox cells transfected with si-Circ_0002111#1 and si-Circ_0002111#2 or negative control siRNA (si-NC) were determined by qRT-PCR and Western blot, respectively. * $P < 0.05$; ** $P < 0.01$.

DUSP14 may interact with miR-557 competitively to regulate each other's expression level.

Hsa_circ_0002111 regulated euthyrox-resistance of PTC cells via miR-557/DUSP14 pathway

Finally, we studied the mechanism of how the role of Circ_0002111 depends on miR-557. We found that knockdown of Circ_0002111 can upregulate miR-557 but downregulate DUSP14, which were restored by the addition of miR-557-inhibitor (Fig. 5a–c). Importantly, knockdown of Circ_0002111 can downregulate the viability of TPC-1/euthyrox and K1/euthyrox after euthyrox treatment at different concentrations (Fig. 5d–f) and upregulated euthyrox-induced apoptosis (Fig. 5g, h), which were both significantly recovered with the addition of miR-557 inhibitor. The above results showed that the regulation of Circ_0002111 euthyrox-resistance of PTC cells depended on the miR-557/DUSP14 signaling pathway.

Discussion

MiRNAs are emerging as a hot topic in cancer therapy (16). Studies have also shown that miRNAs can be a

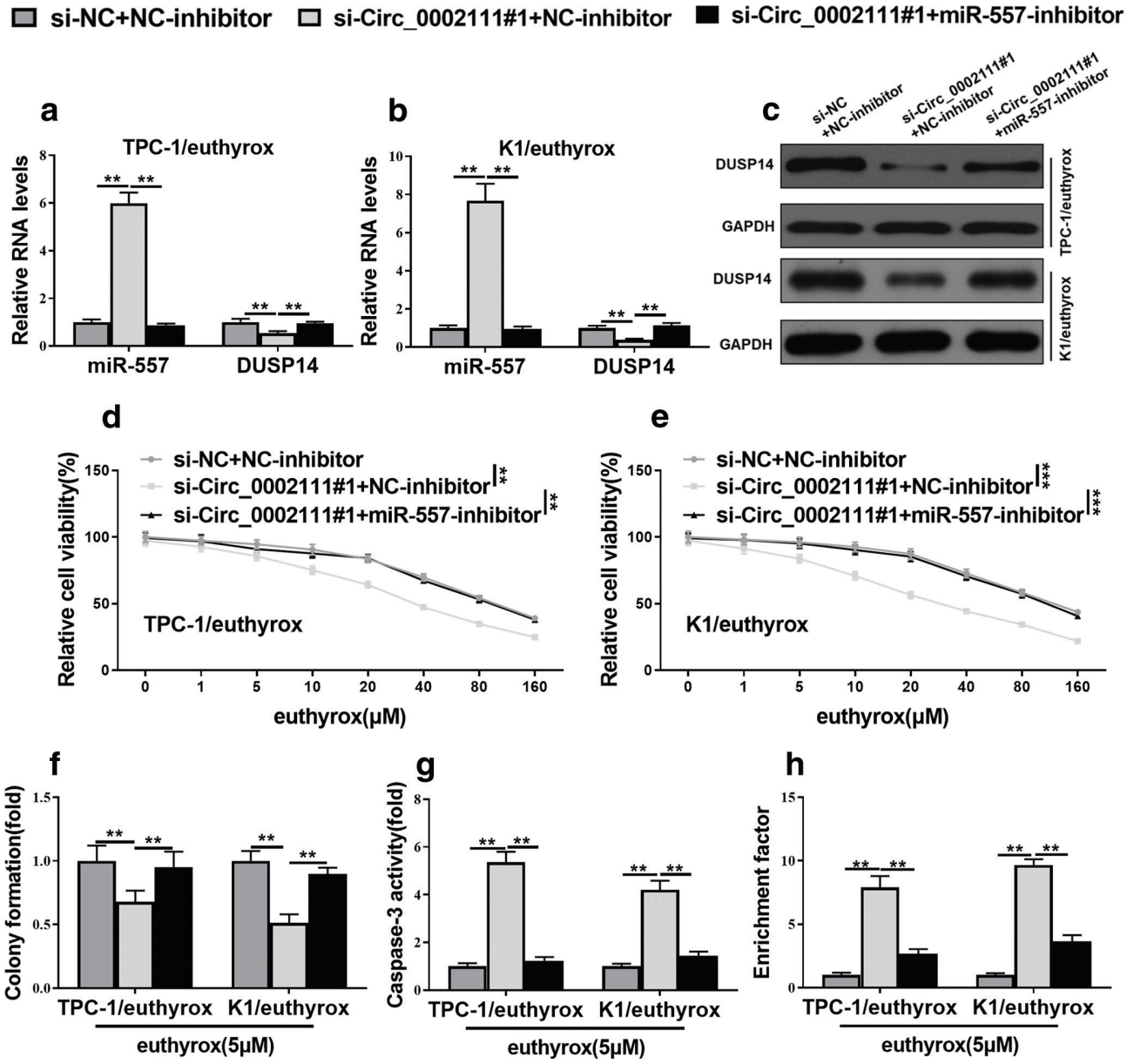

Fig. 5. Hsa_circ_0002111 regulated euthyrox-resistance of PTC cells via miR-557/DUSP14 pathway. TPC-1/euthyrox and K1/euthyrox cells were cotransfected with si-NC+NC-inhibitor, si-Circ_0002111#1+ NC-inhibitor, or si-Circ_0002111#1+ miR-557-inhibitor. (a, b) RNA levels of miR-557 and DUSP14 in the cotransfected TPC-1/euthyrox and K1/euthyrox cells were examined by qRT-PCR. (c) Protein level of DUSP14 in the cotransfected TPC-1/euthyrox and K1/euthyrox cells was determined by Western blot. (d, e) CCK-8 assays were conducted to evaluate the survival rate of the cotransfected TPC-1/euthyrox and K1/euthyrox cells treated with different doses of euthyrox for 48 h. (f) Colony formation assay was performed to determine cell proliferation ability of the cotransfected TPC-1/euthyrox and K1/euthyrox cells with the treatment of euthyrox (5 μM). (g, h) Cell apoptosis of the cotransfected TPC-1/euthyrox and K1/euthyrox cells treated with 5 μM euthyrox was assessed by caspase-3 activity assay and nucleosomal fragmentation assay. * $P < 0.05$; ** $P < 0.01$.

potential marker for diagnosis, evidenced by its application in pancreatic cancer in clinic (17). Circular RNAs are believed to regulate gene expression by sponging RNA-binding proteins and microRNAs (18). As a direct target for Circ_0002111, miR-557 could also be considered as a diagnostic marker for PTC, or its mimics could be a therapeutic candidate. There is no direct evidence in the correlation between miR-557 and PTC overall survival rate, but it has been identified as a tumor suppressor in human lung cancer by regulating LEF1 expression negatively (19) or suppresses the pancreatic cancer cell invasion and proliferation by targeting EGFR (20). These studies further support our result that the inhibition of miR-557 would lead a high survival of tumor cells. In the

future study, it would be interesting to see the relationship of miR-557 with the overall survival rate of PTC, especially those with euthyrox-resistance.

DUSP14 is found to be expressed in epithelial cells (The Human Protein Atlas), and an unfavorable prognostic marker for renal cancer, and also found to have high expression in various cancers, with highest expression in TC (21–24). Its expression pattern is not known in euthyrox-resistant PTC; as we predicted from the mechanism we found through in vitro cell line experiments, it could show a high expression level versus the unresistant PTC. Though it has been identified as a cancer-related gene, it has never been described how it functions in PTC, which makes our finding even interesting. Thus, next, we will further investigate DUSP14 as a potential diagnostic marker or therapeutic target for euthyrox-resistant PTC.

DUSP14 is involved in the inactivation of MAP kinases, dephosphorylates ERK (25), and JNK and p38 MAP-kinases. It has been found that the OTULIN phosphatase limits necroptosis (26), which makes sense that high expression of DUSP14 will lead to high survival of cells. DUSP14 can also rescues apoptosis via the activation of Nrf2 (27), which is an evidence for our finding that knockdown of Circ_0002111 induced apoptosis in PTC cell lines because there is none or decreased miR-557 inhibition, which led to high level of miR-557, which inhibits DUSP14, thus resulted in apoptosis. Further mechanism needs to be clarified how DUSP14 functions in this process.

In drug resistance study, there is always debating whether the defined factor is an induced outcome or the cause for resistance. In our study, we cannot know whether Circ_0002111 is induced by the treatment of euthyrox or it is the cause for euthyrox-resistance. Further study needs to clarify this as to design a clinic study before the use of euthyrox and to follow the outcome through the treatment. Nevertheless, our findings gave a hint that patients with high expression of Circ_0002111 should be treated with more caution while using euthyrox.

Conclusion

Has_Circ_0002111 plays an important role in the sensitivity to euthyrox in PTC cell lines, possibly via targeting DUSP14 through miR-557. It could be a potential target for the treatment of euthyrox-resistant PTC patients.

Acknowledgment

None.

Conflict of interest and funding

None declared.

References

1. Cabanillas ME, McFadden DG, Durante C. Thyroid cancer. Lancet 2016; 388: 2783–95. doi: 10.1016/S0140-6736(16)30172-6
2. Wiltshire JJ, Drake TM, Uttley L, Balasubramanian SP. Systematic review of trends in the incidence rates of thyroid cancer. Thyroid 2016; 26: 1541–52. doi: 10.1089/thy.2016.0100
3. Mao YS, Xing MZ. Recent incidences and differential trends of thyroid cancer in the USA. Endocr Relat Cancer 2016; 23: 313–22. doi: 10.1530/ERC-15-0445
4. Aragon Han P, Weng CH, Khawaja HT, Nagarajan N, Schneider EB, Umbricht CB, et al. MicroRNA expression and association with clinicopathologic features in papillary thyroid cancer: a systematic review. Thyroid 2015; 25: 1322–9. doi: 10.1089/thy.2015.0193
5. Kunavisarut T. Diagnostic biomarkers of differentiated thyroid cancer. Endocrine 2013; 44: 616–22. doi: 10.1007/s12020-013-9974-2
6. Lundgren CI, Hall P, Dickman PW, Zedenius J. Clinically significant prognostic factors for differentiated thyroid carcinoma: a population-based, nested case-control study. Cancer 2006; 106: 524–31. doi: 10.1002/cncr.21653
7. Fiore E, Rago T, Latrofa F, Provenzale MA, Piaggi P, Delitala A, et al. Hashimoto's thyroiditis is associated with papillary thyroid carcinoma: role of TSH and of treatment with L-thyroxine. Endocr Relat Cancer 2011; 18: 429–37. doi: 10.1530/ERC-11-0028
8. Han B, Chao J, Yao HH. Circular RNA and its mechanisms in disease: from the bench to the clinic. Pharmacol Ther 2018; 187: 31–44. doi: 10.1016/j.pharmthera.2018.01.010
9. Nicolet BP, Engels S, Aglialoro F, van den Akker E, von Lindern M, Wolkers MC. Circular RNA expression in human hematopoietic cells is widespread and cell-type specific. Nucleic Acids Res 2018; 46: 8168–80. doi: 10.1093/nar/gky721
10. Salzman J. Circular RNA Expression: its potential regulation and function. Trends Genet 2016; 32: 309–16. doi: 10.1016/j.tig.2016.03.002
11. Jin XY, Wang ZY, Pang WY, Zhou J, Liang Y, Yang JJ, et al. Upregulated hsa_circ_0004458 contributes to progression of papillary thyroid carcinoma by inhibition of miR-885-5p and activation of RAC1. Med Sci Monit 2018; 24: 5488–500. doi: 10.12659/MSM.911095
12. Tian XF, Zhang L, Jiao Y, Chen JS, Shan Y, Yang WF. CircABCB10 promotes nonsmall cell lung cancer cell proliferation and migration by regulating the miR-1252/FOXR2 axis. J Cell Biochem 2019; 120: 3765–72. doi: 10.1002/jcb.27657
13. Yao Y, Chen XY, Yang H, Chen W, Qian YC, Yan ZY, et al. Hsa_circ_0058124 promotes papillary thyroid cancer tumorigenesis and invasiveness through the NOTCH3/GATAD2A axis. J Exp Clin Cancer Res 2019; 38: 318. doi: 10.1186/s13046-019-1321-x
14. Li QD, Wang YC, Wu S, Zhou Z, Ding XJ, Shi RH, et al. CircACC1 regulates assembly and activation of AMPK complex under metabolic stress. Cell Metab 2019; 30: 157–73.e7. doi: 10.1016/j.cmet.2019.05.009
15. Zhao HD, Tang HL, Huang QK, Qiu B, Liu XM, Fan D, et al. MiR-101 targets USP22 to inhibit the tumorigenesis of papillary thyroid carcinoma. Am J Cancer Res 2016; 6: 2575–86.
16. Wang Z. Editorial (hot topic: miRNAs as legitimate targets for cancer therapy). Curr Drug Targets 2013; 14: 1093. doi: 10.2174/1389450111314100001
17. Shao H, Zhang Y, Yan J, Ban X, Fan X, Chang X, et al. Upregulated MicroRNA-483-3p is an early event in pancreatic ductal adenocarcinoma (PDAC) and as a powerful liquid biopsy biomarker in PDAC. Onco Targets Ther 2021; 14: 2163–75. doi: 10.2147/OTT.S288936
18. Panda AC. Circular RNAs act as miRNA sponges. Adv Exp Med Biol 2018; 1087: 67–79. doi: 10.1007/978-981-13-1426-1_6

19. Qiu J, Hao Y, Huang S, Ma Y, Li X, Li D, et al. MiR-557 works as a tumor suppressor in human lung cancers by negatively regulating LEF1 expression. Tumour Biol 2017; 39: 1010428317709467. doi: 10.1177/1010428317709467
20. Yang Y, Sun KK, Shen XJ, Wu XY, Li DC. miR-557 inhibits the proliferation and invasion of pancreatic cancer cells by targeting EGFR. Int J Clin Exp Pathol 2019; 12: 1333–41.
21. Kia V, Paryan M, Mortazavi Y, Biglari A, Mohammadi-Yeganeh S. Evaluation of exosomal miR-9 and miR-155 targeting PTEN and DUSP14 in highly metastatic breast cancer and their effect on low metastatic cells. J Cell Biochem 2019; 120: 5666–76. doi: 10.1002/jcb.27850
22. Mabrouk NMK, Elkaffash DM, Abdel-Hadi M, Abdelmoneim SE, Saad ElDeen S, Gewaifel G, et al. Identification of the possible therapeutic targets in the insulin-like growth factor 1 receptor pathway in a cohort of Egyptian hepatocellular carcinoma complicating chronic hepatitis C type 4. Drug Target Insights 2020; 14: 1–11. doi: 10.33393/dti.2020.1548
23. Wei Y, Wang G, Wang C, Zhou Y, Zhang J, Xu K. Upregulation of DUSP14 affects proliferation, invasion and metastasis, potentially via epithelial-mesenchymal transition and is associated with poor prognosis in pancreatic cancer. Cancer Manag Res 2020; 12: 2097–108. doi: 10.2147/CMAR.S240040
24. Yan F, Ying L, Li X, Qiao B, Meng Q, Yu L, et al. Overexpression of the transcription factor ATF3 with a regulatory molecular signature associates with the pathogenic development of colorectal cancer. Oncotarget 2017; 8: 47020–36. doi: 10.18632/oncotarget.16638
25. Ashraf S, Hegazy YK, Harmancey R. Nuclear receptor subfamily 4 group A member 2 inhibits activation of ERK signaling and cell growth in response to beta-adrenergic stimulation in adult rat cardiomyocytes. Am J Physiol Cell Physiol 2019; 317: C513–24. doi: 10.1152/ajpcell.00526.2018
26. Douglas T, Saleh M. Post-translational modification of OTULIN regulates ubiquitin dynamics and cell death. Cell Rep 2019; 29: 3652–63.e5. doi: 10.1016/j.celrep.2019.11.014
27. Jianrong S, Yanjun Z, Chen Y, Jianwen X. DUSP14 rescues cerebral ischemia/reperfusion (IR) injury by reducing inflammation and apoptosis via the activation of Nrf-2. Biochem Biophys Res Commun 2019; 509: 713–21. doi: 10.1016/j.bbrc.2018.12.170

***Pengxin Zhao**
No. 215 Heping West Road
Shijiazhuang 050000, China
Email: zhaopengxin@hb2h.com